BNL-107767-2015-JA

Bouncing Alkaline Batteries: A Basic Solution

S. Bhadra,[1] B.J. Hertzberg,[2] M. Croft,[3] J.W. Gallaway,[4] B.J. Van Tassell,[5] M. Chamoun,[6] C. Erdonmez,[6] Z. Zhong,[7] and D.A. Steingart[2]

[1] *Electrical Engineering and the Andlinger Center for Energy and The Environment, Princeton University, Princeton, New Jersey 08540, USA*[*]

[2] *Mechanical and Aerospace Engineering and the Andlinger Center for Energy and The Environment, Princeton University,Princeton, New Jersey 08540, USA*[†]

[3] *Department of Physics, Rutgers University, Piscataway, New Jersey 08854, USA*[‡]

[4] *City University of New York Energy Institute, New York, New York 10031, USA*[§]

[5] *Department of Chemical Engineering, City College of New York, New York, New York 10031, USA*[¶]

[6] *Sustainable Technologies Division, Brookhaven National Laboratory, Upton, New York 11973, USA*[**]

[7] *National Synchrotron Light Source, Brookhaven National Laboratory, Upton, New York 11973, USA*[††]

(Dated: July 23, 2014)

The coefficient of restitution of alkaline batteries has been shown to increase as a function of depth of discharge. In this work, using non-destructive mechanical testing, the change in coefficient of restitution is compared to *in situ* energy-dispersive x-ray diffraction data to determine the cause of the macroscopic change in coefficient of restitution. The increase in coefficient of restitution correlates to the formation of a percolation pathway of ZnO within the anode of the cell, and that the coefficient of restitution saturates at a value of 0.63 ± .05 at 50% state of charge when the anode has densified into porous ZnO solid. Of note is the sensitivity of coefficient of restitution to the amount of ZnO formation that rivals the sensitivity of *in situ* energy-dispersive x-ray diffraction spectroscopy.

PACS numbers: 81.70.Cv, 82.45.Jn, 82.45.Fk, 82.47.Cb

[*] sbhadra@princeton.edu
[†] bhertzberg3@gmail.com
[‡] croft@physics.rutgers.edu
[§] joshuagallaway@gmail.com
[¶] bajavata@gmail.com
[**] myladchamoun@gmail.com
[††] zhong@bnl.gov

The LR6 form factor $Zn-MnO_2$ battery, or the "alkaline" AA battery accounts for $1.8 billion in worldwide battery sales in 2013 [1, 2]. The chemistry and form factor have been popular for over 50 years because of the low cost of both the source materials (Zn and MnO2) and the bobbin cell design. [3] Electrical testing is the accepted method of determining a battery's health, but mechanical testing of batteries has surfaced as a viable method for determining the material properties of a battery. Methods have probed the mechanical behavior of the separator [4, 5], the electrodes [6–10], and the entire cell [11]. The destructive nature of some of these methods makes them unfeasible for applications in which the cell must remain intact. Methods such as X-ray diffraction (XRD) [12], X-ray microtomography [13–15], and acoustic emission sensing [16–19] allow for non-destructive *in situ* characterization of the microstructure, but both methods require specialized equipment and, with few exceptions, cannot be applied *in operando*.

Recently, there has been popular interest [20] in the tendency of an alkaline AA battery to bounce after being dropped on its end when discharged to full capacity, compared to a flat landing with minimal bounce when the battery is "as-received". In this paper the coefficient of restitution (COR) of an alkaline AA battery is measured at various depths of discharge by dropping the battery in a controlled fashion and observing the subsequent bouncing. Our measurements show that this simple bounce test can provide a considerable amount of information of the structure of the battery's Zn anode, rivaling the sensitivity of *in situ* energy-dispersive x-ray spectroscopy (EDXRD) in detection of ZnO formation. This discovery shows that non-destructive acoustic testing of batteries can provide valuable information about a battery's health and state of charge (SOC).

To measure the COR of each Duracell Coppertop LR6 alkaline AA battery, the batteries were dropped through a 25 cm tall acrylic tube onto an epoxy benchtop, coupled with a computer microphone placed 30 cm away to record the audio from each bounce, similar to the method of Stensgaard et al [21]. The audio recording was then analyzed to determine number of bounces, height of bounce, and COR. The height of each bounce was determined by the relationship

$$\mathrm{h_{bounce}}=\tfrac{1}{2}\mathrm{g}(\frac{\Delta t_{bounce}}{2})^2 \tag{1}$$

where $\Delta \mathrm{t_{bounce}}$ is the time measured between bounces with the microphone. The batteries were weighed with a lab balance (Metler-Toledo) prior to each bounce test to determine total weight, which remained constant at 23.05 ± 0.1 g. Batteries were then discharged for one hour at 280 mA, corresponding to a rate of C/10 (1/10 of capacity per hour) using a battery cycler (Neware BT3000-8) after each bounce test.

Electrochemical impedance spectroscopy (Gamry Reference 3000) was performed on each cell after every 280 mAh of capacity discharge. Scans were performed under potentiostatic conditions at the open circuit voltage of each cell, with an AC voltage perturbation of 10 mV, sweeping from 100 mHz to 100 kHz. EIS and bounce test data was then compared to *in situ* EDXRD data obtained at Beamline X17B1 of the National Synchrotron Light Source at Brookhaven National Laboratory. EDXRD is capable of measuring internal structural changes in a discrete volume, and a method detailed by Gallaway et al[12] was employed.

As an alkaline battery is discharged, the anode undergoes oxidation from Zn to ZnO, as seen in Eq. 2 and 3, while the cathode is reduced from MnO_2 to MnOOH, shown in Eq. 4.

$$\mathrm{Zn} + 4\,\mathrm{OH^-} \longrightarrow \mathrm{Zn(OH)_4^{2-}} + 2\,\mathrm{e^-} \tag{2}$$

$$\mathrm{Zn(OH)_4^{2-}} \longrightarrow \mathrm{ZnO} + \mathrm{H_2O} + 2\,\mathrm{OH^-} \tag{3}$$

$$\mathrm{MnO_2} + \mathrm{H_2O} + \mathrm{e^-} \longrightarrow \mathrm{MnOOH} + \mathrm{OH^-} \tag{4}$$

Equation 2 shows that the battery produces $\mathrm{Zn(OH)_4^{2-}}$ ions in solution until the electrolyte becomes supersaturated, at which point it begins to precipitate as ZnO [22].

Post mortem analysis shows that the Zn gel anode densifies into porous, ZnO solid, as shown in the SEM micrographs in Fig. 1. The densification of the anode affects the mechanical properties of the battery. The COR, which measures the elasticity of a collision between an object and a rigid object, is one such mechanical property that can be determined as shown in Eq. 5.

$$\mathrm{COR}=\sqrt{\frac{h_2}{h_1}} \tag{5}$$

where h_1 is the drop height, and h_2 is the maximum bounce height determined from Eq. 1. Using the bounce test described previously, the COR of alkaline batteries was measured through full discharge.

Figure 2 shows the evolution of the COR for three identical AA cells as capacity is passed in increments of 280 milliamp-hours (mAh), corresponding to a rate of C/10. A sharp increase in COR occurs at 80% SOC, when 560 mAh have passed, followed by saturation of the COR at a value of 0.63 ± 0.05 at 50% SOC (1400 mAh passed). The three cells show excellent agreement in the low and high COR regimes, and the variance in the dynamic regime (80% to 50% SOC) shows that there is some variance from cell to cell in ZnO growth.

To show the transition between the low COR and high COR regimes more clearly, cells were discharged at 50 mA in one hour intervals (50 mAh) prior to bounce testing. It was found that COR is constant for low depths of discharge, rising after 450 mAh have been passed (see the Supplemental Material [23]). The saturation for these cells occured at 950 mAh passed, which was earlier than in cells discharged at 280 mA. It has been shown previously by Horn et al [24] that lower discharge rates will result in a more even distribution of ZnO in the anode, compared to that of a higher discharge rate, thus a more even distribution of ZnO results in earlier saturation of the COR.

Four possible effects associated with discharging an alkaline battery may be correlated with the observed change in COR: 1) water consumption, 2) mass loss, 3) reduction of the cathode from MnO_2 to MnOOH, and 4) oxidation of the anode from Zn to ZnO. To discount water consumption, which occurs as water is consumed at the cathode and sequestered in the ZnO that forms, the positive terminal of two AA cells were removed, and the cells were dehydrated in a vacuum oven at 25C for 72 hours to remove water from the KOH electrolyte. Overall, 2.3 g of water were lost from each cell. Table I illustrates that water content has no measurable effect on COR before or after discharge. Mass loss can be discounted as well, as under all operating conditions, no change was observed in the mass of each battery. Therefore, the structural changes associated with the oxidation of the zinc anode must be the major contribution to the increased COR of the alkaline cell. The EDXRD spectra for the MnO_2 cathode shows peak shifts that begin immediately upon discharge, at least 400 mAh before the onset of COR increase (see Supplemental Material [23]). In addition, assuming a full extent of reaction, the reduction of the MnO_2 only results in a 23% increase in volume whereas oxidation of the Zn results in a 60% volume change. Thus, the reduction of the cathode can be discounted as a mechanism contributing to the increase in the COR [25].

TABLE I. Water content effect on coefficient of restitution

	Coefficient of restitution at 100% SOC	Coefficient of restitution at 0% SOC
As received	0.1 ± 0.05	0.43 ± 0.02
Dehydrated	0.1 ± 0.05	0.42 ± 0.02

One method for measuring the evolution of interfaces within a battery is electrochemical impedance spectroscopy (EIS) [26, 27]. EIS was performed after every 10% of capacity discharged (280 mAh) to observe the effects of anode oxidation on the impedance of the battery. We found a high reactance (Z") and resistance (Z') in the as-received battery, with a two order of magnitude drop in both Z" and Z' following 10% discharge of the cell (see the Supplemental Material [23]). This drop was most evident in the low frequency regime of the EIS spectra, often associated with mass transport limitations. We believe this high initial impedance of the cell is related to a proprietary polymeric coating on the zinc anode used in this brand of battery to improve the shelf life. It was confirmed that while other brands

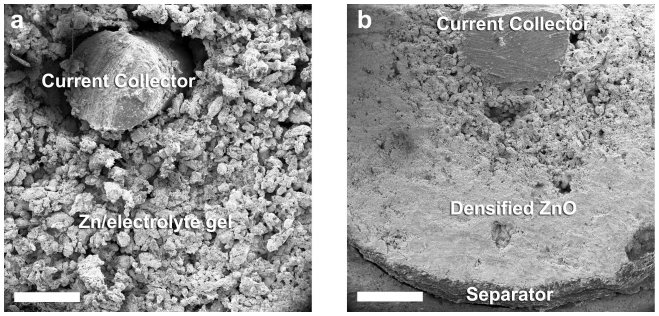

FIG. 1. a) SEM image of "as-received" cell, where the coarse zinc/electrolyte gel can be seen surrounding the current collector. b) SEM image of the same cell after full discharge (2850 mAh passed), the anode now largely converted to ZnO. A density gradient can be seen, with the region of compact growth closest to the separator. Scale bar = 1 mm

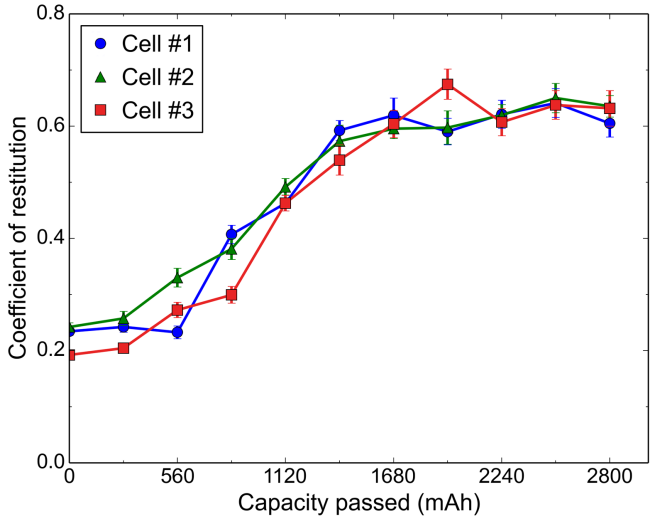

FIG. 2. (color online). Coefficient of restitution as a function of capacity passed. COR increases at 80% state of charge, and saturates at 50% state of charge.

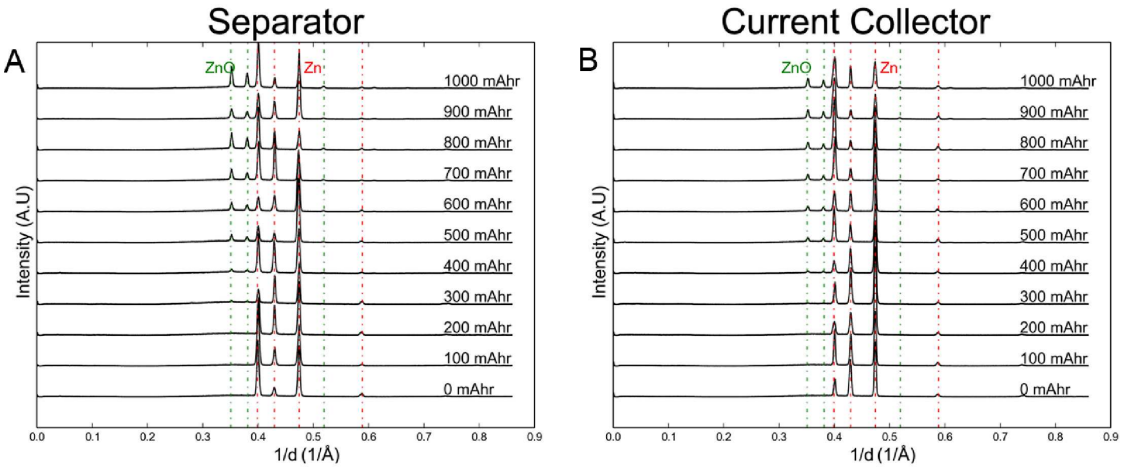

FIG. 3. (color online). XRD progression of anode at 100 mA discharge rate at the a) anode/separator interface and b) anode/current collector interfaces. ZnO peaks are denoted by green dashed lines, and Zn peaks are denoted by red dashed lines. ZnO forms at the separator before forming at the current collector.

of AA alkaline batteries do not have this high initial electrochemical impedance, they do exhibit the same increase in COR as a function of depth of discharge.

EIS suggests that some structural evolution occurs within the anode, but a method is required to characterize discrete volumes within the battery to understand the oxidation process. Recent studies have shown that performing *in situ* EDXRD on batteries during discharge can probe the evolution of the internal components [12–14]. Using similar methods, *in situ* EDXRD was performed in AA batteries at three discharge rates: 100 mA, 200 mA, and 300 mA. EDXRD allows for collection of spatially resolved data, which allows imaging of the oxidation of Zn to ZnO at both edges of the anode: the separator and the current collector. Fig. 3a shows that ZnO forms at the separator interface before forming at the current collector interface, shown in Fig. 3b. This trend holds for all three discharge rates (see the Supplemental Material [23]). The capacity passed at which ZnO is present at each interface is detailed in Table II.

These spectra confirm the results of Horn et al [24], who have shown that at higher discharge rates, ZnO will grow preferentially at the separator interface before growing through the anode towards the current collector. They have found that ZnO initially grows as a shell around the Zn particles (Type I ZnO) through solution-precipitation of $Zn(OH)_4^{2-}$. Once the particle is completely enveloped in Type I ZnO it begins to oxidize and deposit onto the the inside surface of the Type I ZnO shell via a second solution-precipitation step (Type II ZnO). Based on the EDXRD spectra in Fig. 3, it can be shwon that the oxidation of the cell ultimately forms a percolation network of

TABLE II. Formation of ZnO within the anode

Discharge rate (mA)	Capacity passed before appearance of ZnO at separator (mAh)	Capacity passed before appearance of ZnO at current collector (mAh)
100	200 - 300	300 - 400
200	200 - 400	400 - 600
300	300 - 600	300 - 600

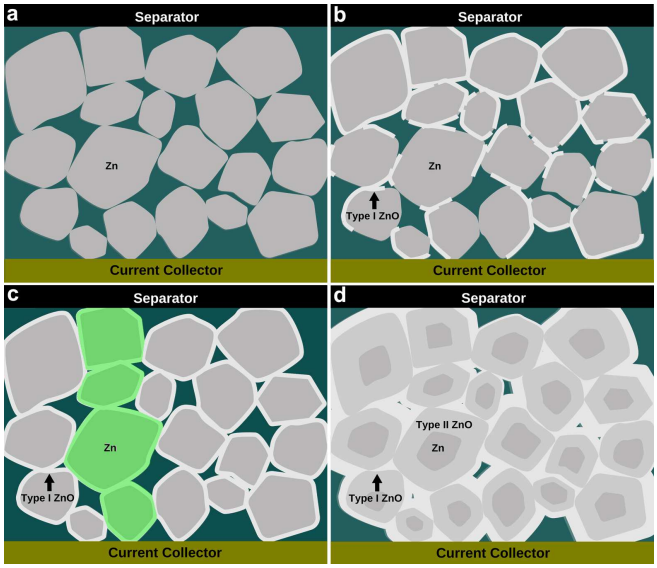

FIG. 4. (color online). The progression of ZnO formation in the anode. a) The initial anode gel comprised of Zn particles in an electrolyte/cellulose matrix. b) Formation of Type I ZnO shells on Zn particles. Oxidation occurs preferentially at the separator. c) Formation of a percolation pathway. As all particles become clad in ZnO shells, a contiguous network of ZnO-clad particles forms from separator to current collector (highlighted in green). d) Densification of the anode. Type I ZnO shells grow and Zn particles oxidize to Type II ZnO.

ZnO from the separator to the current collector. This agrees well with the results of Arise et al. [28], who have shown that following initial precipitation of ZnO onto the anode surface, the particles will coarsen and form dense films. Comparing the bounce test data presented in Fig. 2 with the EDXRD spectra in Fig. 3, it is clear that the formation of this percolation pathway occurs at the same time that the COR increases. This hypothesis is supported by the use of ZnO as an industrial additive to increase the COR of materials [29], and previous studies performed on ceramic/metal composites (cermets) [30], in which increasing the ceramic content of a cermet will result in an increase in the COR, assuming the ceramic has a higher elastic modulus relative to the metal matrix. Treating the partially oxidized anode as a cermet, and knowing that ZnO has an elastic modulus of 140 GPa relative to 108 GPa for bulk Zn, leading to an increase in COR as the Zn particles are oxidized [31]. The saturation of COR is best explained using the methods of Antonyuk et al. [32], who have found that a material's COR will saturate at the point at which it no longer yields plastically. Using Faradaic analysis, 1400 mAh passed (50% SOC), 1.71 g of Zn will be consumed at the anode, while 2.13 g of ZnO will be produced. At this state of charge half the Zn has been converted to ZnO, assuming a zinc limited battery, making ZnO the majority phase in the anode, both volumetrically and gravimetrically. As per Horn et al and Arise et al. [24, 28], the Type I ZnO shells will form together and sequester the liquid electrolyte, while the bulk of the Zn particle will be oxidized to Type II ZnO. Initially, the anode gel consists of discrete Zn particles that can move within the gel matrix. Once percolation begins, this motion becomes suppressed. Once the anode densifies, as shown in Figure 1b, it becomes a stiff ceramic core that arrests all movement of the discrete Zn particles, and the COR saturates. This process is detailed in Fig. 4, which shows the initial gel, the growth of Type I ZnO, the percolation of ZnO in the anode, and the final densification of the anode.

In conclusion, it is shown that determination of the COR of an alkaline battery through a simple bounce test provides an accurate measure of the state of charge of the battery. The bounce test functions as a measure of the bulk properties of a battery, as it depends on the level of oxidation of the Zn anode. Percolation of ZnO through the anode

was determined to be the cause of an increase in the COR, while densification of the anode into a ZnO solid resulted in the saturation of the COR. The sensitivity of the bounce test data relative to the EDXRD data surprising, as the bounce test is capable of determining the percolation of ZnO in the anode to within 13% of the EDXRD determined value. This work shows that unconventional means of mechanical battery testing can offer knowledge of the health of a battery system at a fraction of the cost and the complexity of established methods. The bounce test is a start, as future methods could incorporate a transducer/detector system in which the acoustic characteristics of a cell could be measured *in situ* without interruption of the battery system operation.

We are grateful for the patience of the Steingart lab as this work had to be carried out in a completely silent environment. We also acknowledge Sonny Moore for his contributions to drop testing in electro-acoustic applications. This work was performed with financial support from the National Science Foundation CMMI 1402872, Department of Energy ARPA-E RANGE DE-AR0000400, and the Laboratory Directed Research and Development Program of Brookhaven National Laboratory (LDRD-BNL) under Contract No. DE-AC02-98CH 10866 with the U.S. Department of Energy. Use of the National Synchrotron Light Source, Brookhaven National Laboratory, was supported by the U.S. Department of Energy, Office of Science, Office of Basic Energy Sciences, under Contract No. DE-AC02-98CH10886.

[1] Highbeam Business, "Primary batteries, dry and wet market report,".
[2] "Battery manufacturing in the US," Retrieved February 28, 2014, from `http://clients1.ibisworld.com/reports/us/industry/default.aspx?entid=801`.
[3] K. Karl, P. A. Marsal, and L. F. Urry, U. S. Patent No. 2,960,558 (Nov 15, 1960).
[4] J. Cannarella and C. B. Arnold, J. Power Sources **226**, 149 (2013).
[5] C. Peabody and C. B. Arnold, J. Power Sources **196**, 8147 (2011).
[6] Y.-H. Chen, C.-W. Wang, X. Zhang, and A. Sastry, J. Power Sources **195**, 2851 (2010).
[7] W. Du, A. Gupta, X. Zhang, A. M. Sastry, and W. Shyy, Int. J. Heat Mass Transfer **53**, 3552 (2010).
[8] S. Han, J. Park, W. Lu, and A. M. Sastry, J. Power Sources **240**, 155 (2013).
[9] J. Park, S. Kalnaus, S. Han, Y. K. Lee, G. B. Less, N. J. Dudney, C. Daniel, and A. M. Sastry, J. Power Sources **222**, 417 (2013).
[10] K. Striebel, A. Sierra, J. Shim, C.-W. Wang, and A. Sastry, J. Power Sources **134**, 241 (2004).
[11] J. Cannarella and C. B. Arnold, J. Power Sources **245**, 745 (2014).
[12] J. W. Gallaway, C. K. Erdonmez, Z. Zhong, M. Croft, L. A. Sviridov, T. Z. Sholklapper, D. E. Turney, S. Banerjee, and D. A. Steingart, J. Mater. Chem. A **2**, 2757 (2014).
[13] A. Haibel, I. Manke, A. Melzer, and J. Banhart, J. Electrochem. Soc. **157**, A387 (2010).
[14] I. Manke, J. Banhart, A. Haibel, A. Rack, S. Zabler, N. Kardjilov, A. Hilger, A. Melzer, and H. Riesemeier, Appl. Phys. Lett. **90**, 214102 (2007).
[15] M. Ebner, F. Marone, M. Stampanoni, and V. Wood, Science **342**, 716 (2013).
[16] A. Etiemble, H. Idrissi, S. Meille, and L. Rou, J. Power Sources **205**, 500 (2012).
[17] S. Kalnaus, K. Rhodes, and C. Daniel, J. Power Sources **196**, 8116 (2011).
[18] N. Kircheva, S. Genies, C. Chabrol, and P.-X. Thivel, Electrochim. Acta **88**, 488 (2013).
[19] K. Rhodes, M. Kirkham, R. Meisner, C. M. Parish, N. Dudney, and C. Daniel, Rev. Sci. Instrum. **82**, 075107 (2011).
[20] "How to test a AA battery," Retrieved March 25, 2014 from `http://www.youtube.com/watch?v=Y_m6p99l6ME`.
[21] I. Stensgaard and E. Lgsgaard, Am. J. Phys. **69**, 301 (2001).
[22] T. Reddy, *Linden's Handbook of Batteries, 4th Edition* (McGraw-Hill Education, 2010).
[23] See Supplemental Material at [URL will be inserted by publisher] for detailed methods, testing setup and audio data.
[24] Q. C. Horn and Y. Shao-Horn, J. Electrochem. Soc. **150**, A652 (2003).
[25] W. Roberts, T. Campbell, and G. Rapp, *Encyclopedia of minerals* (Van Nostrand Reinhold, 1990).
[26] D. A. Dornbusch, R. Hilton, M. J. Gordon, and G. J. Suppes, ECS Electrochem. Lett. **2**, A89 (2013).
[27] R. K. Ghavami, Z. Rafiei, and S. M. Tabatabaei, J. Power Sources **164**, 934 (2007).
[28] I. Arise, S. Kawai, Y. Fukunaka, and F. R. McLarnon, J. Electrochem. Soc. **160**, D66 (2013).
[29] R. D. Nesbitt and M. J. Sullivan, U. S. Patent No. 6,142,887 (Nov 7, 2000).
[30] I. Hussainova, J. Kbarsepp, and I. Shcheglov, Tribol. Int. **32**, 337 (1999).
[31] C. Q. Chen, Y. Shi, Y. S. Zhang, J. Zhu, and Y. J. Yan, Phys. Rev. Lett. **96**, 075505 (2006).
[32] S. Antonyuk, S. Heinrich, J. Tomas, N. G. Deen, M. S. Buijtenen, and J. A. M. Kuipers, Granul. Matter **12**, 15 (2010).